Title	Application of empirical mode decomposition to drive-by bridge damage detection
Authors(s)	O'Brien, Eugene J.; Malekjafarian, Abdollah; González, Arturo
Publication date	2017-01
Publication information	European Journal of Mechanics, A/Solids, 61 : 151-163
Publisher	Elsevier
Item record/more information	http://hdl.handle.net/10197/8780
Publisher's statement	þÿ T h i s i s t h e a u t h o r s v e r s i o n o f a w o r k t h a t w a s a c c e p t e d f o Journal of Mechanics, A/Solids. Changes resulting from the publishing process, such as peer review, editing, corrections, structural formatting, and other quality control mechanisms may not be reflected in this document. Changes may have been made to this work since it was submitted for publication. A definitive version was subsequently published in European Journal of Mechanics, A/Solids, 61 2017-01, pp.151-163. DOI: 10.1016/j.euromechsol.2016.09.009
Publisher's version (DOI)	10.1016/j.euromechsol.2016.09.009

Application of Empirical Mode Decomposition to Drive-by Bridge Damage Detection

Eugene J. OBrien[1], Abdollah Malekjafarian[2*], Arturo González[3]

[1] Professor, email: eugene.obrien@ucd.ie
School of Civil Engineering and Earth Institute, University College Dublin, Ireland
[2] Postdoctoral researcher, email: abdollah.malekjafarian@ucd.ie
School of Civil Engineering, University College Dublin, Ireland
[3] Lecturer, email: Arturo.gonzalez@ucd.ie
School of Civil Engineering, University College Dublin, Ireland

[*] Corresponding author. Postal address: School of Civil Engineering, University College Dublin, Newstead, Belfield, Dublin 4, Ireland.
Phone number: +353 1 7163229.
Email address: abdollah.malekjafarian@ucd.ie, a.malekjafarian@gmail.com

Abstract

A new method is proposed in this paper for bridge damage detection using the response measured in a passing vehicle. It is shown theoretically that such a response includes three main components; vehicle frequency, bridge natural frequency and a vehicle speed pseudo-frequency component. The Empirical Mode Decomposition (EMD) method is used to decompose the signal into its main components. A damage detection method is proposed using the Intrinsic Mode Functions (IMFs) corresponding to the vehicle speed component of the response measured on the passing vehicle. Numerical case studies using Finite Element modelling of Vehicle Bridge Interaction are used to show the performance of the proposed method. It is demonstrated that it can successfully localise the damage location in the absence of road profile. A difference in the acceleration signals of healthy and corresponding damaged structures is used to identify the damage location in the presence of a road profile. The performance of the method for changes in the transverse position of the vehicle on the bridge is also studied.

Key words: Bridge; Damage detection; Indirect method

1. Introduction

Bridges play a key role in road and rail transportation. However, concrete and steel deteriorate over time and many bridges in the developed world are structurally deficient. Therefore bridge condition monitoring is becoming a key element in the planning of maintenance interventions in transport infrastructure. Today, visual inspections are widely used for bridge damage detection. While effective in many cases, visual inspection suffers variability in the judgments of inspectors and accessibility issues which may leave some types of damage undiscovered.

In recent years, there has been an increasing interest in vibration-based structural health monitoring methods for bridge damage detection. These approaches are mainly based on the variation of modal parameters of the structure (i.e. natural frequency, mode shape and damping ratio) with structural health condition. Natural frequency change is the most common damage indicator, but it is generally accepted that natural frequencies alone cannot provide local information about damage (Fan and Qiao, 2011). Recently more sensitive modal parameters such as mode shapes and modal curvatures have gained attention. These approaches have the potential to provide local information on the structural condition of the structure (Fan and Qiao, 2011).

Although these vibration-based methods can provide high quality information about bridge condition, they require the installation of many sensors and access to electrical power on the bridge. Considering the large number of short and medium span bridges, the instrumentation becomes expensive and smaller bridges are not routinely instrumented at this point in time. Recently, this drawback of direct methods has led to the concept of an indirect approach in which bridge condition is investigated using data measured on a passing vehicle (Malekjafarian et al., 2015). The idea is first proposed to extract the bridge natural frequency from indirect measurements (Yang et al., 2004). It is shown that the acceleration response measured on a vehicle passing over the bridge includes enough bridge response to reveal the bridge natural

frequencies. Early research in this field is focused on the validation of the idea experimentally (Lin and Yang, 2005), improvement of the accuracy (Kim and Kawatani, 2009; Yang and Chen, 2015; Yang and Chang, 2009a) and accessing bridge natural frequencies other than just the first one (Yang and Chang, 2009b). Recent research investigates other modal parameters such as damping ratio (González et al., 2012) and mode shapes (Malekjafarian and Obrien, 2014; Oshima et al., 2014; Yang et al., 2014). Yang et al. (2014) show that the bridge mode shape can be identified from the Hilbert amplitude of a filtered response measured on a passing axle. Oshima et al. (2014) propose a method in which the bridge mode shapes are found from the response measured on a truck-trailer system. The mode shapes are identified by applying Singular Value Decomposition (SVD) to the responses measured on several axles of the truck-trailer system. Malekjafarian and Obrien (2014) propose Short Time Frequency Domain Decomposition (STFDD) for the identification of bridge mode shapes from the response measured on two following axles passing over the bridge. It is shown that the mode shapes can be constructed by applying Frequency Domain Decomposition (FDD) to the responses in a multi-step procedure.

Several attempts have been made to detect bridge damage using indirect measurements (Kim et al., 2014; Lederman et al., 2014; Li and Au, 2014; McGetrick and Kim, 2014a; Nguyen and Tran, 2010). Nguyen and Tran (2010) use a Symlet wavelet transform of the displacement response measured on a moving vehicle to identify the location of cracks in a bridge. McGetrick and Kim (2013); McGetrick and Kim (2014b) apply a Continuous Wavelet Transform (CWT) to the dynamic response of a passing vehicle. It is demonstrated that the CWT coefficients are affected when the axle passes over a damaged section. Li and Au (2014) suggest a multistage damage detection approach using modal strain energy and the genetic algorithm (GA). The approach successfully detects the location of damage in a two-span continuous bridge. OBrien and Keenahan (2014) introduce a new drive-by damage detection method using the concept of the apparent road profile. A mode-shape based damage detection method is proposed in (OBrien

and Malekjafarian, 2016) using an improved version of the STFDD method. They obtain a better resolution of the bridge mode shapes which has good potential for damage detection.

In this paper, the theoretical response of a vehicle passing over a bridge is presented first. It is shown in (Yang et al., 2004) that the response measured on a passing vehicle contains three main components; vehicle frequency, bridge natural frequency and the pseudo frequency associated with vehicle speed. The first of these relates to the vehicle dynamic response and the last two correspond to the bridge response. Generally, those components corresponding to the bridge dynamics reflect the bridge condition. He and Zhu (2015) investigate the dynamic response of a bridge to a moving load (which is generally a moving vehicle). They show that the pseudo-frequency component of the response is more sensitive to damage and is preferred for damage localization. This finding is used in this paper, by separating the pseudo-frequency component of the response and using it for damage detection. The Empirical Mode Decomposition (EMD) is applied to the axle response to decompose it into different components using a sifting process. It is shown that the damage location can be detected using the IMFs corresponding to the pseudo-frequency. A finite element (FE) model of Vehicle Bridge Interaction (VBI) is used to provide a numerical case study to validate the method. A simulation of a quarter car passing over a bridge with a smooth road surface is followed by a case with good road roughness. Finally, the sensitivity of the method to changes in the transverse position of the vehicle on the bridge is investigated.

2. Theoretical background

The basis of indirect bridge monitoring is to use the response measured on a passing vehicle. A comprehensive theoretical look at this response is necessary for a better understanding of the indirect approach. A closed-form VBI solution is presented in this section to identify the main components of the response measured on a passing vehicle.

2.1. The response measured on a passing vehicle

A greatly simplified model is first considered to identify the basic features of the system. The vehicle is modelled as a sprung mass and the bridge as a simply supported beam considering only the first mode. Then, the equation of motion for the sprung mass moving over the beam, shown in Fig. 1 can be written as (Yang et al., 2004):

$$m_v\ddot{q}_v + k_v(q_v - u|_{x=vt}) = 0 \tag{1}$$

where q_v is the vertical displacement of the sprung mass, m_v and k_v are the mass and stiffness of the sprung mass and u is the beam deflection. By considering the contact force between the sprung mass and the beam and the beam displacement due to the moving load, Eq. 1 can be expressed as (Yang et al., 2004):

$$m_v\ddot{q}_v + ({\omega_v}^2 m_v)q_v - \left[{\omega_v}^2 m_v \sin\left(\frac{\pi v t}{L}\right)\right] q_b = 0 \tag{2}$$

where ω_v is the sprung mass natural frequency given by $\omega_v = \sqrt{\frac{k_v}{m_v}}$, v is the speed of the sprung mass, t is time, L is the total length of the beam and q_b is the deflection at mid-span of the beam.

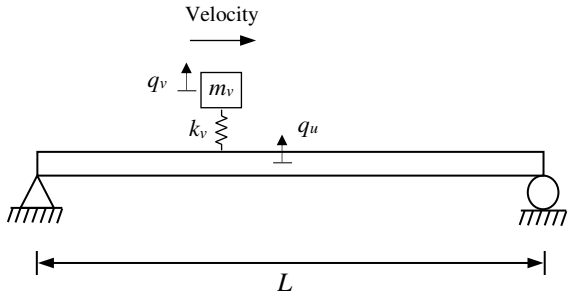

Figure 1: A sprung mass passing over a bridge

If the vehicle mass is much less than the total mass of the bridge, then the vehicle displacement can be approximated as (Yang et al., 2004):

$$q_v(t) = \frac{\Delta_{st}}{2(1-S^2)}\left[(1 - cos\omega_v t) - \frac{cos2\pi vt/L - cos\omega_v t}{1-(2\mu S)^2} - S\frac{cos(\omega_b - \pi v/L)\,t - cos\omega_v t}{1-\mu^2(1-S)^2} + S\frac{cos(\omega_b + \pi v/L)\,t - cos\omega_v t}{1-\mu^2(1+S)^2}\right] \tag{3}$$

where μ is the the ratio of the bridge frequency to the vehicle frequency, $\mu = \omega_b/\omega_v$, Δ_{st} is the approximate static deflection at mid-span of the beam under the gravity action of the mass m_v at that point and S is defined as $S = {}^{\pi v}/_{L\omega_b}$. This can be calculated using:

$$\Delta_{st} = -\frac{2m_v g L^3}{\pi^4 EI} \tag{4}$$

where g is the acceleration due to gravity, E is the elastic modulus and I is the second moment of area.

The acceleration of the moving vehicle can be obtained by differentiating Eq. 3 twice (Yang et al., 2004):

$$\begin{aligned}\ddot{q}_v(t) = \frac{\Delta_{st}{\omega_v}^2}{2(1-S^2)}\Bigg[&cos\omega_v t + \frac{(2\mu S)^2 cos2\pi vt/L - cos\omega_v t}{1-(2\mu S)^2} \\ &+ S\frac{\mu^2(1-S)^2\, cos(\omega_b - \pi v/L)\, t - cos\omega_v t}{1-\mu^2(1-S)^2} \\ &- S\frac{\mu^2(1+S)^2\, cos(\omega_b + \pi v/L)\, t - cos\omega_v t}{1-\mu^2(1+S)^2}\Bigg]\end{aligned} \tag{5}$$

For a better understanding of the different components of vehicle acceleration, Eq. 5 can be rewritten as:

$$\ddot{q}_v(t) = \frac{\Delta_{st}{\omega_v}^2}{2(1-S^2)}\left[A_1 cos\omega_v t + A_2 cos\frac{2\pi v}{L}t + A_3 cos\left(\omega_b - \frac{\pi v}{L}\right)t + A_4 cos\left(\omega_b + \frac{\pi v}{L}\right)t\right] \tag{6}$$

where A_1, A_2, A_3 and A_4 determine the relative contributions of each component to the total acceleration response. These are given by:

$$A_1 = 1 - \frac{1}{1-(2\mu S)^2} - \frac{S}{1-\mu^2(1-S)^2} + \frac{S}{1-\mu^2(1+S)^2} \tag{7}$$

$$A_2 = \frac{(2\mu S)^2}{1-(2\mu S)^2}$$

$$A_3 = \frac{S\mu^2(1-S)^2}{1-\mu^2(1-S)^2}$$

$$A_4 = \frac{S\mu^2(1+S)^2}{1-\mu^2(1+S)^2}$$

From Eq. 6, three main components exists in the total response that can be written as:

$$\ddot{q}_{v_{veh}}(t) = \frac{\Delta_{st}{\omega_v}^2}{2(1-S^2)} A_1 cos\omega_v t \tag{8}$$

$$\ddot{q}_{v_{spe}}(t) = \frac{\Delta_{st}{\omega_v}^2}{2(1-S^2)} A_2 cos\frac{2\pi v}{L} t$$

$$\ddot{q}_{v_{br}}(t) = \frac{\Delta_{st}{\omega_v}^2}{2(1-S^2)} \left[A_3 cos\left(\omega_b - \frac{\pi v}{L}\right) t + A_4 cos\left(\omega_b + \frac{\pi v}{L}\right) t\right]$$

where $\ddot{q}_{v_{veh}}$ is the component associated with the vehicle frequency, $\ddot{q}_{v_{spe}}$ is that part of the signal associated with vehicle speed and $\ddot{q}_{v_{br}}$ is the component associated with the bridge natural frequency.

A simple case study is considered here to demonstrate the different components of the vehicle response. A mass-spring system with properties of $m_v = 700$ kg and $k_v = 1.75\times10^6$ N/m is travelling over a simply supported beam with the properties given in Table 1. The vehicle speed is 10 m/s.

Table 1. Properties of the bridge

Properties	Unit	Symbol	value
Length	m	L	15
Mass per unit length	kg/m	m	28125
Modulus of elasticity	N/mm^2	E	35000
Second moment of area	m^4	J	0.5273
First natural frequency	Hz	ω_b	5.65

The acceleration of the moving axle is calculated using Eq. 5 and is shown in Fig. 2 (a). The Fast Fourier Transform (FFT) of the acceleration is plotted in Fig. 2 (b) and shows the dominant frequencies in the response. As was expected from Eq. 5, the response consists of three main components, the frequencies of which are numbered in the FFT spectrum: (1) the speed pseudo-frequency, (2) the bridge frequency and (3) the vehicle frequency (Yang et al., 2004).

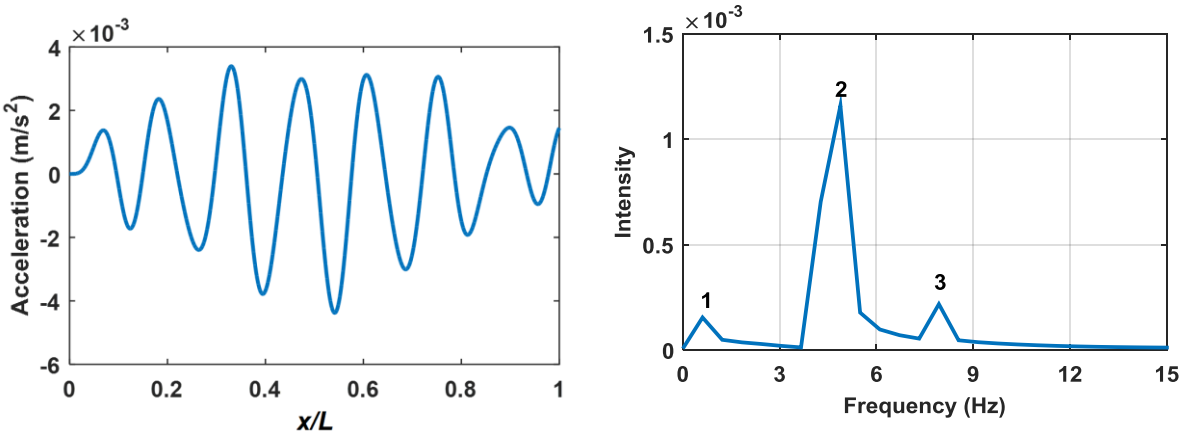

Figure 2: The response measured on a passing vehicle; (a) total acceleration, (b) FFT of the acceleration ($x/L = vt/L$).

For a better understanding of the response, each component is plotted separately in Fig. 3. Fig. 3(a) shows the speed pseudo-frequency part of the response which is related to the vehicle speed and the total length of the bridge. Fig. 3(b) shows the bridge vibrations measured on the vehicle. As only the first mode of the bridge is considered in the closed-form solution, this part only presents the first mode shape, corresponding to the first natural frequency of the bridge. Finally Fig. 3(c) shows the vehicle's free vibrations.

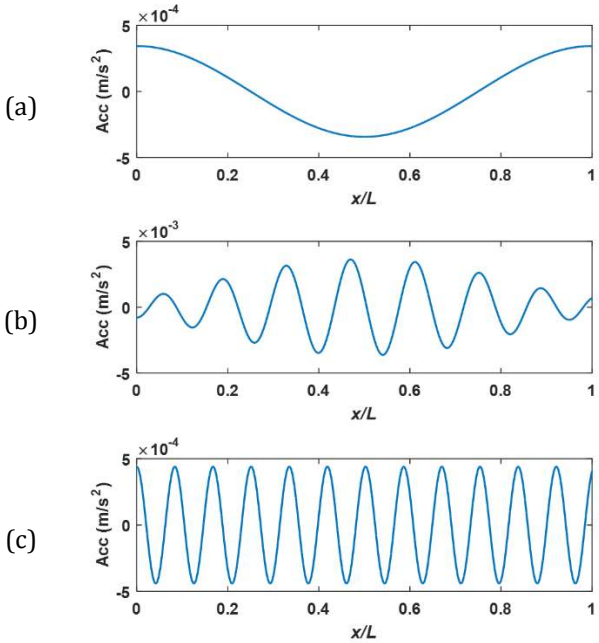

Figure 3: Components of the acceleration response; (a) speed pseudo-frequency part; (b) bridge frequency part and (c) vehicle frequency part ($x/L = vt/L$).

For monitoring purposes, the bridge components of the indirect response are of interest. Many researchers have carried out studies on indirect bridge monitoring that consider bridge component in the measured response. These methods are usually based on the fact that damage to the bridge causes a change in its dynamic properties such as natural frequencies, damping ratios and mode shapes. By identifying these properties from the response measured on the vehicle, it is possible to investigate the bridge's health condition. The most common method is detecting changes in the bridge natural frequencies which could be observable in the FFT of the response measured on the vehicle, $\ddot{q}_v$ which originally comes from $\ddot{q}_{v_{br}}$. Some researchers believe that natural frequency is not a sufficiently sensitive parameter for damage detection and may be affected by environmental conditions such as temperature (Fan and Qiao, 2011; Qiao and Cao, 2008). For this reason, using other parameters such as bridge mode shape has been suggested. Recently, some new methods have been proposed for the identification of bridge mode shapes using indirect measurements (Malekjafarian and Obrien, 2014; OBrien and Malekjafarian, 2015; Yang et al., 2014). The concept behind these methods is that the bridge frequency component of the vehicle response includes the full mode shapes of the bridge as the vehicle is measuring this part of the response on a moving coordinate system. On the other hand, there are some publications that consider the measured signal directly, seeking a discontinuity at the damage location using methods such as the Wavelet transform. The basis behind these methods can be understood by looking at the bridge response. It is shown in (He and Zhu, 2015) that the speed pseudo-frequency part of the response is very sensitive to damage when the response is measured directly on the bridge. The same explanation can be given for indirect measurements. Therefore, it can be concluded that if the response measured on a passing vehicle can be decomposed into its original components, the speed pseudo-frequency part can show the damage location.

2.2. Empirical Mode Decomposition (EMD)

The EMD method (Huang et al., 1999; Huang et al., 1998) is a new signal processing tool which decomposes any signal, non-stationary or even nonlinear, into several so-called Intrinsic Mode

Functions (IMFs). It has been used before for damage detection and structural health monitoring (Chen et al., 2014; Kurt et al., 2012). The procedure of extracting an IMF is called sifting and is as follows:

1. Identify all the local maxima and minima in the original time signal.
2. Connect all the local maxima and minima with cubic splines as the upper and lower envelopes.
3. Compute the mean value of the two envelopes and subtract it from the original signal.

The differences between the original time history and the mean value is the IMF, if it satisfies the following conditions: the number of extrema and the number of zero crossings must be equal or differ at most by one and at any point the mean value of the envelope defined by the local maxima and the envelope defined by the local minima must be zero. The sifting procedure continues until the residue becomes so small that it is less than a predetermined value of consequence, or the residue becomes a monotonic function. The original time signal can then be expressed as the sum of the IMFs and the final residue. The first IMF contains the highest frequency content of the original signal and the final residue contains the lowest frequency in the signal.

The bridge displacement and acceleration responses are obtained by theoretical calculation explained in Section 2.1. The EMD method is used in this section to decompose the theoretical responses. It is observed that in the case that the acceleration response is considered, the method works better when the vehicle frequency is removed from the total signal by using a moving average filtering (MAF). Therefore, before applying EMD, a MAF is set to the vehicle frequency and applied to the acceleration signal to remove the vehicle component from the total response measured on the vehicle. The IMFs obtained from the EMD and their FFT spectra are shown in Figs. 4 and 5 for displacement and acceleration respectively. It can be understood from the FFT spectrum of the first IMF that it is associated with the bridge first natural frequency (5.65 Hz) which is shifted by the vehicle speed. The second and third IMFs are related

to the speed pseudo-frequency part of the signal. Therefore, by removing the first IMF from the original signal, the speed pseudo-frequency part which was previously shown to be sensitive to damage, can be extracted from the signal.

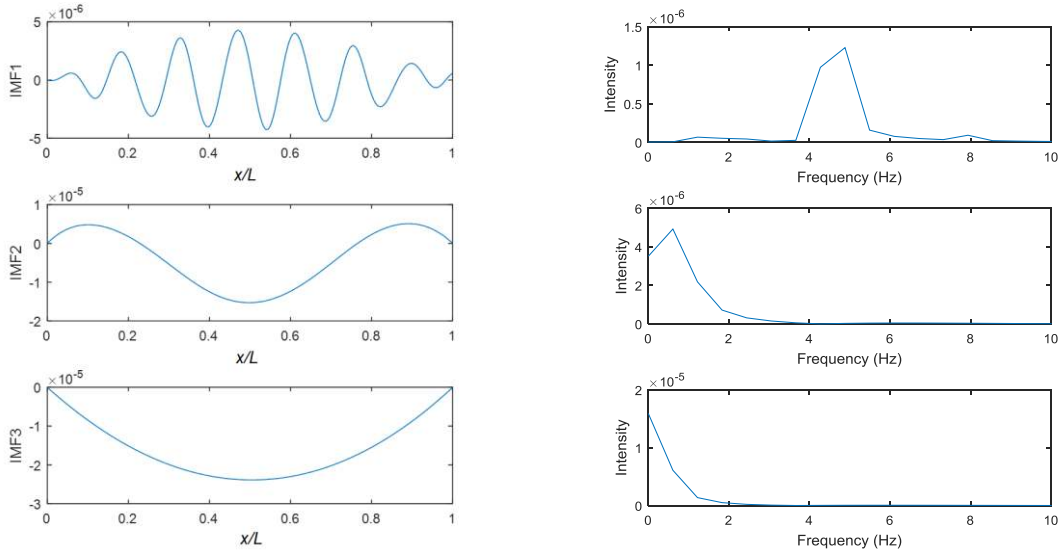

Figure 4: IMFs of the vehicle displacement response and their FFT spectra ($x/L = vt/L$).

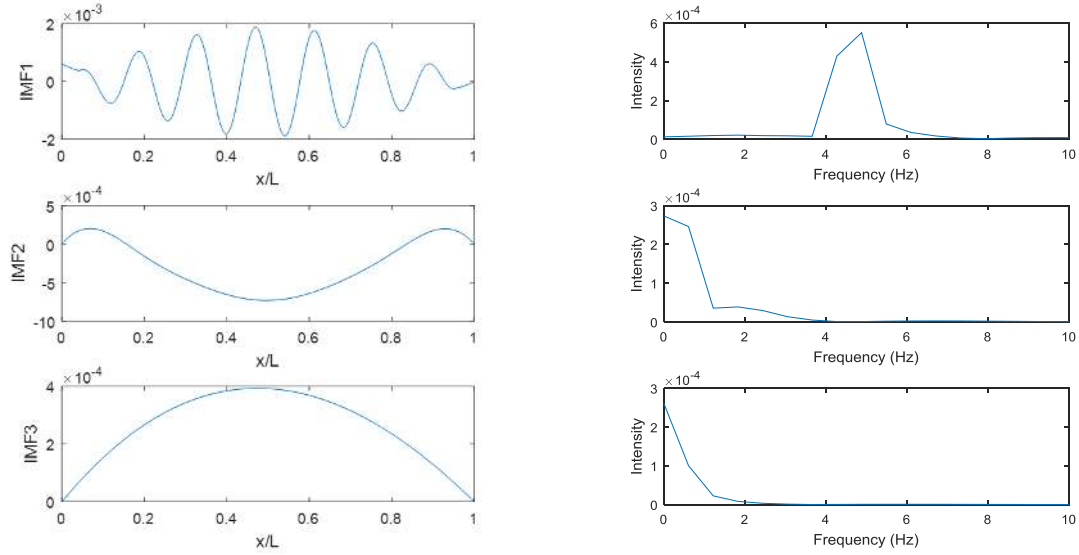

Figure 5: IMFs of the filtered vehicle acceleration response and their FFT spectra ($x/L = vt/L$).

Figs. 6(a) and 6(b) show sum of the second and third IMFs obtained from the displacement and acceleration responses respectively. It can be seen that they are similar to the speed pseudo-frequency part of the original signal shown in Fig. 3.

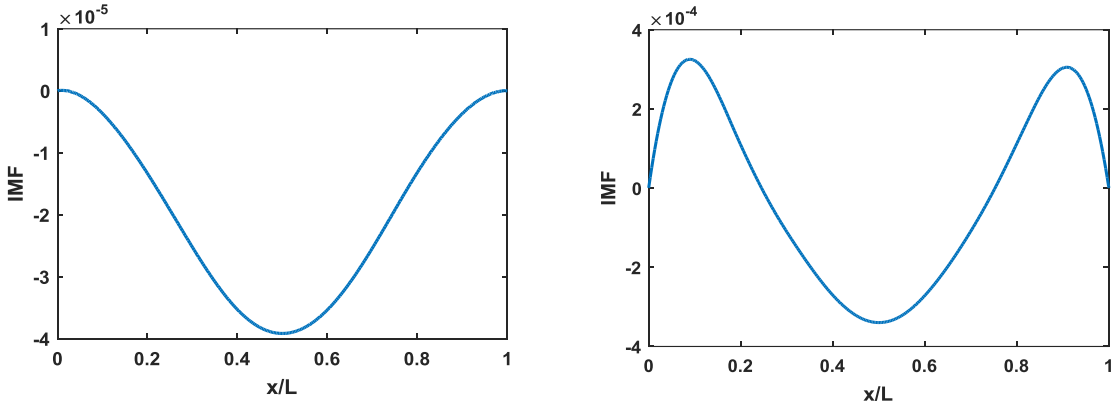

Figure 6: Sum of the second and third IMFs. (a) Displacement and (b) acceleration ($x/L = vt/L$).

3. Numerical modelling

3.1. Finite Element modelling of Vehicle Bridge Interaction

A Finite Element (FE) Vehicle Bridge Interaction (VBI) model is used here according to the procedure used by Malekjafarian and Obrien (2014). In this model, a coupled VBI system is represented and the solution is calculated at each time step using an iterative procedure. The quarter-car model shown in Fig. 7 is used in this paper as it illustrates many of the important characteristics of VBI (Cebon, 1999). The vehicle has two independent degrees of freedom corresponding to body mass and axle mass translations. The vehicle body and axle component masses are represented by m_s and m_u and their displacements by y_s and y_u respectively. The axle mass is connected to the road surface via a spring with linear stiffness k_t which represents the tyre. By imposing equilibrium of all forces and moments acting on the vehicle masses, the equations of motion of the vehicle model can be obtained in terms of the degrees of freedom:

$$M_v\ddot{y}_v + C_v\dot{y}_v + K_v y_v = f_{int} \tag{9}$$

where M_v, C_v and K_v are the respective mass, damping and stiffness matrices of the vehicle and $\ddot{y}_v$, $\dot{y}_v$ and y_v are the respective vectors of nodal acceleration, velocity and displacement ($y_v = [y_s \quad y_u]^T$). The vector f_{int} contains the time-varying dynamic interaction forces applied to the vehicle degrees of freedom.

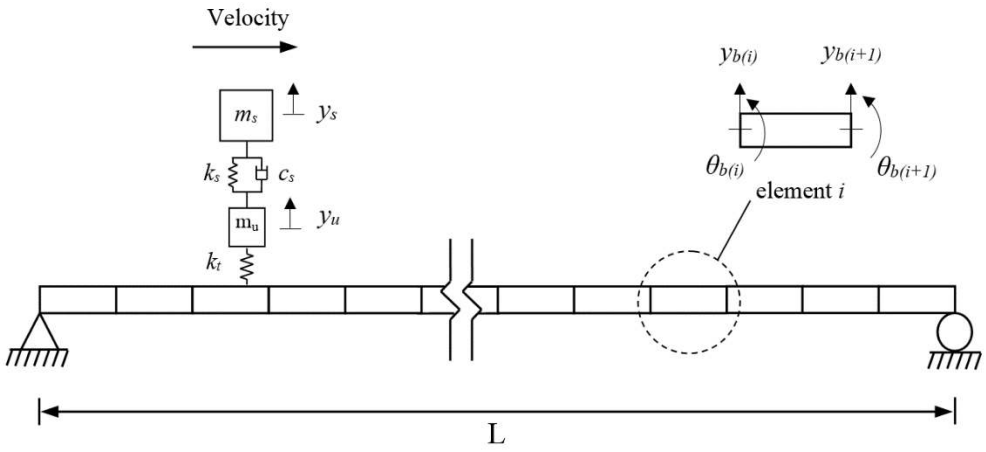

Figure 7: FE model of a quarter car passing over a bridge

The bridge is modelled as a simply supported beam with total span length L using beam finite elements (Tedesco et al., 1999) (Fig. 7). Each beam element is represented by four degrees of freedom (one translational and one rotational for each of two nodes), constant mass per unit length, m, modulus of elasticity, E and second moment of area, J. The equations of motion of the beam under a series of moving time-varying forces can be written in terms of its degrees of freedom:

$$M_b\ddot{y}_b + C_b\dot{y}_b + K_b y_b = f_{int} \tag{10}$$

where M_b, C_b and K_b are the global mass, damping and stiffness matrices of the beam model, respectively and $\ddot{y}_b$, $\dot{y}_b$ and y_b are the vectors of nodal bridge accelerations, velocities and translation, respectively. For the case of low bridge damping, ξ, Rayleigh damping can be adopted to represent viscous damping and is given by (Clough and Penzien, 1993):

$$C_b = \alpha M_b + \beta K_b \tag{11}$$

where α and β are constants. The damping ξ is assumed to be proportional for all modes and α and β are obtained from, $\alpha = 2\xi\omega_1\omega_2/(\omega_1 + \omega_2)$ and $\beta = 2\xi/(\omega_1 + \omega_2)$ where ω_1 and ω_2 are the first two natural frequencies of the bridge (Clough and Penzien, 1993). The dynamic interaction between the vehicle and the bridge is implemented in MATLAB. The vehicle and the

bridge are coupled at the tyre contact points via the interaction force vector. Combining equations (9) and (10), the coupled equation of motion of the vehicle and bridge is formed as:

$$M_g\ddot{u} + C_g\dot{u} + K_g u = F \tag{12}$$

where M_g and C_g are the combined system mass and damping matrices, respectively, K_g is the coupled time-varying system stiffness matrix and F is the system force vector. The vector, $u = \{y_v, y_b\}^T$, is the displacement vector of the system. The Wilson-Theta integration scheme (Tedesco et al., 1999) is used to solve the equations for the coupled system with the optimal value of the parameter θ =1.420815 for unconditional stability in the integration scheme. The initial condition of the solution is considered to be zero vertical translation, velocity and acceleration in all simulations.

A quarter-car with the properties given in Table 2 is modelled to pass over a bridge with the same properties given in Table 1. The bridge is modelled using 20 elements. The vehicle speed is 10 m/s and a smooth road profile is considered in this example.

Table 2. Properties of the quarter-car

Properties	Unit	Symbol	Value
Body mass	kg	m_s	9300
Axle mass	kg	m_u	700
Suspension stiffness	N/m	k_s	4×10^5
Suspension damping	Ns/m	c_s	10^4
Tyre stiffness	N/m	k_t	1.75×10^6
Body bounce frequency	Hz	ω_b	0.94
Axle hop frequency	Hz	ω_a	8.83

The first damage case is defined by imposing a crack in the 14th element of the bridge using the crack modelling method proposed by Sinha et al. (2002). Accordingly, the crack is deemed to cause a stiffness loss in a region on each side of it, with the flexibility varying linearly on each side from the uncracked to the cracked beam section. The severity of the damage is represented

by the crack depth, expressed as a ratio of the beam depth. A crack ratio of 0.3 is considered in this example. The vehicle is simulated to pass over the healthy and damaged bridges and the acceleration responses in the axle for each simulation are presented in Fig. 8.

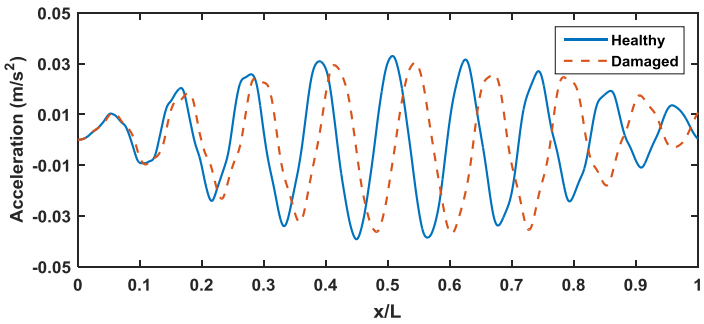

Figure 8: The acceleration measured on the axle ($\ddot{y}_u$) of the vehicle passing over healthy and damaged bridges ($x/L = vt/L$).

3.2. Results for a quarter car on a smooth road profile

The acceleration and displacement responses measured on the vehicle are decomposed into IMFs using EMD (Fig. 9). As introduced in Section 2, the speed pseudo-frequency components of the vehicle responses are extracted from the total response. The responses extracted in this way for both the healthy and damaged cases are compared in Fig. 10 for displacement and acceleration. The damage location is shown by a vertical line. There is a clear difference between the healthy and damaged IMFs, confirming that it is damage-sensitive. Furthermore, the crack location (the vertical blue) aligns quite well with a peak in the differences between the healthy and damaged IMFs. This suggests that, not only can damage be detected, but the location of the damage might also be estimated.

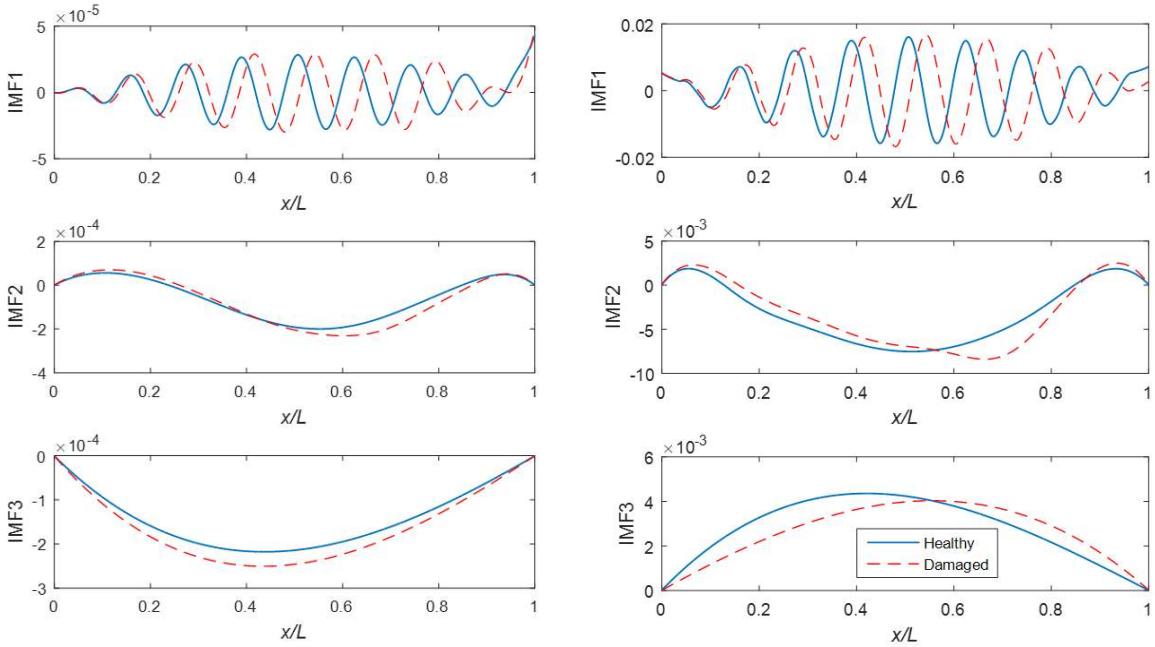

Figure 9: IMFs of the vehicle response. (a) Displacement and (b) acceleration.

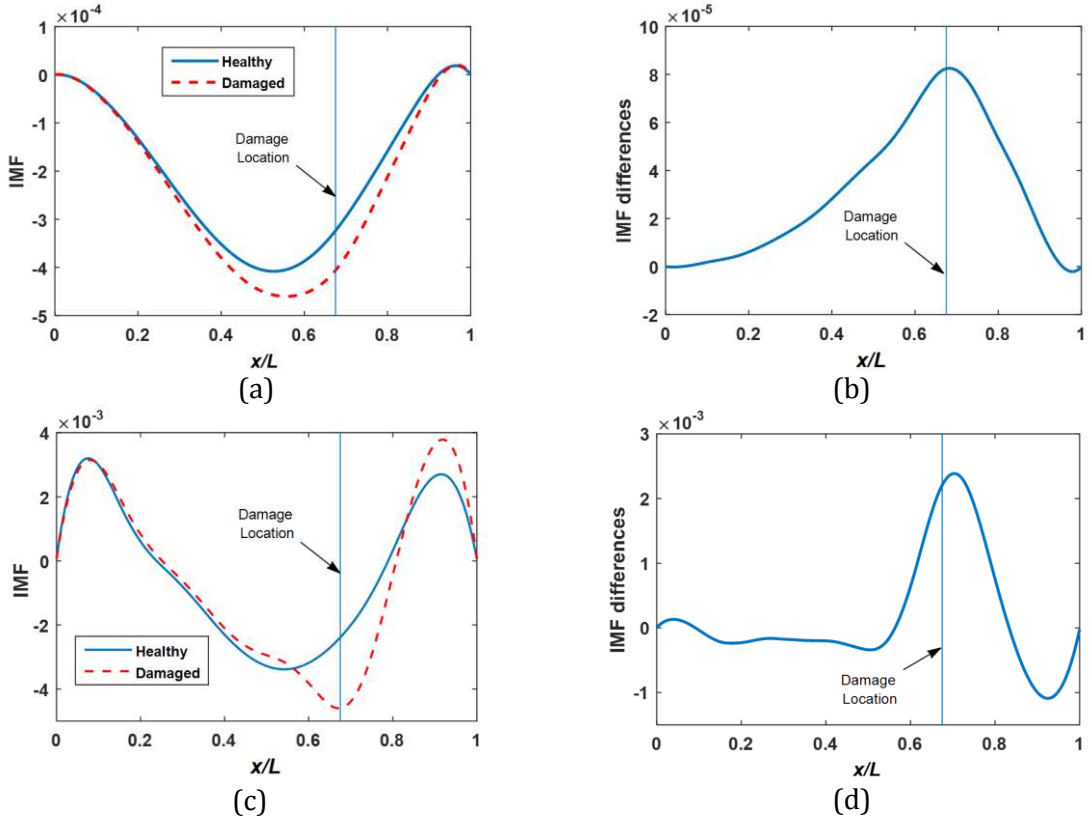

Figure 10: Speed pseudo-frequency component of vehicle response. (a) Comparison of healthy and damaged bridges for displacement and (b) their difference. (c) Comparison of healthy and damaged bridges for acceleration and (d) their difference ($x/L = vt/L$).

To validate the effectiveness of the method for other damage locations, a second damage case is investigated using a new crack location. The new crack has the same depth as the first but is located in the 10th element of the 20 that make up the bridge. The IMFs are obtained for this case and shown in Fig. 11. A comparison of the speed pseudo-frequency components of the vehicle displacements and accelerations for the healthy and the damage cases is presented in Fig. 12. While there is a peak in the difference near the damage location, there are also peaks at other locations with no obvious association. As they appear only in the case considering the acceleration signal, they might be due to the 'end effect' caused by using the MAF. It should be noted that when the displacement signal is considered (Fig. 10 (b)), the proposed method provides more consistent results, having only one peak. On the other hand, when acceleration is considered (Fig. 10(d)), a more local effect is achieved corresponding to damage location, but there are still some peaks due to other effects. It may limit the method to the case that both acceleration and displacement signals may need to be required.

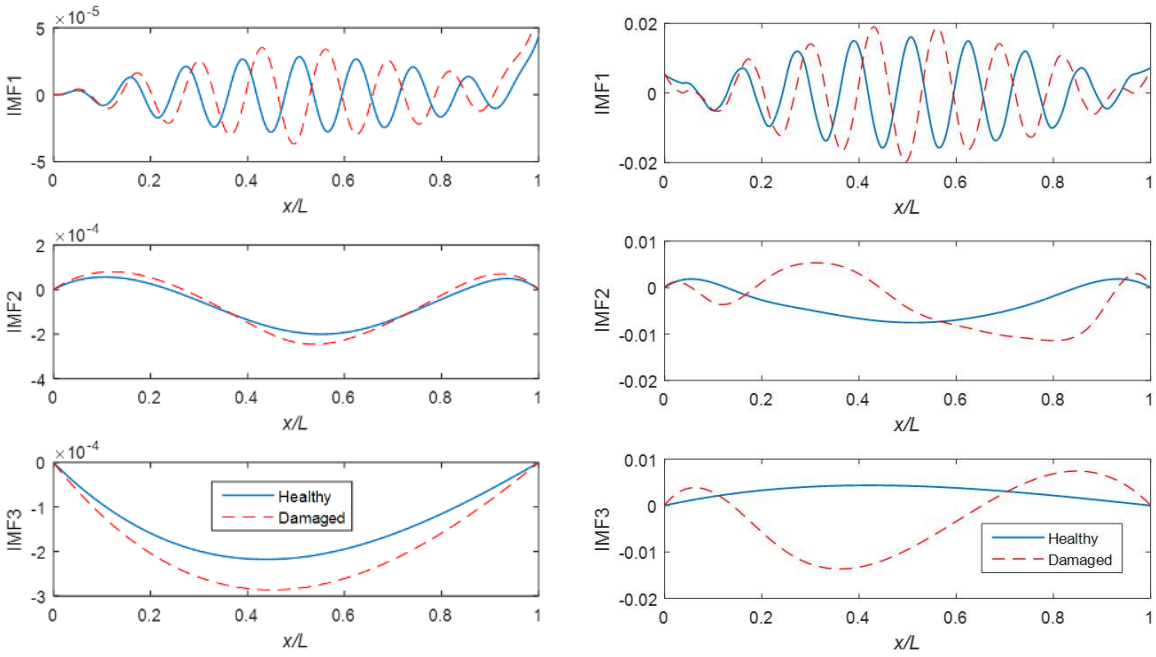

Figure 11: IMFs of the vehicle response. (a) Displacement and (b) acceleration.

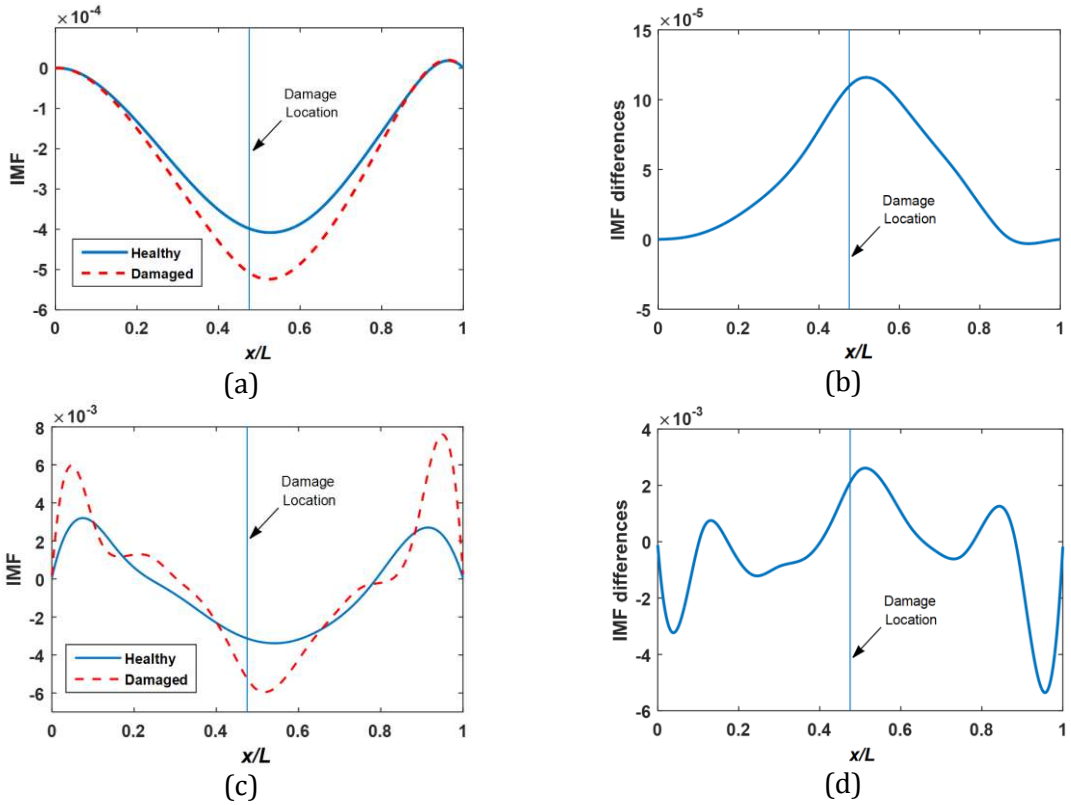

Figure 12: Speed pseudo-frequency components of the accelerations for damage in 10th element. (a) Displacement signal components for the healthy and damaged cases and (b) their difference. (c) Acceleration signal components for the healthy and damaged cases and (d) their difference ($x/L = vt/L$).

3.3. IMF-based Damage indicator

As shown in section 3.2, the difference between the speed pseudo-frequency parts of the acceleration signals for the healthy and damaged structures is sensitive to damage. In this section an IMF-based damage indicator, i.e., a parameter sensitive to damage, is introduced that addresses the contamination introduced by the road surface profile. As shown schematically in Fig. 13, the EMD is applied here to the *difference* between the acceleration signals for the healthy ($\ddot{y}_v^{he}(t)$) and damaged ($\ddot{y}_v^{da}(t)$) structures. The hypothesis is that this subtraction will remove the effects of road profile excitation which are assumed to be similar in the two cases.

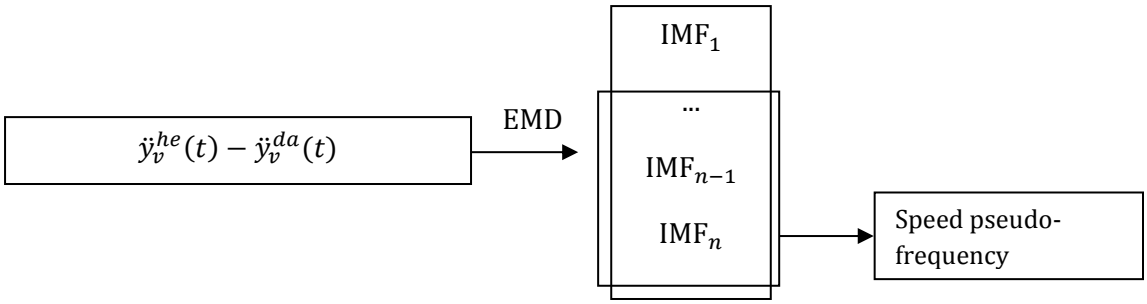

Figure 13: Schematic of damage detection procedure

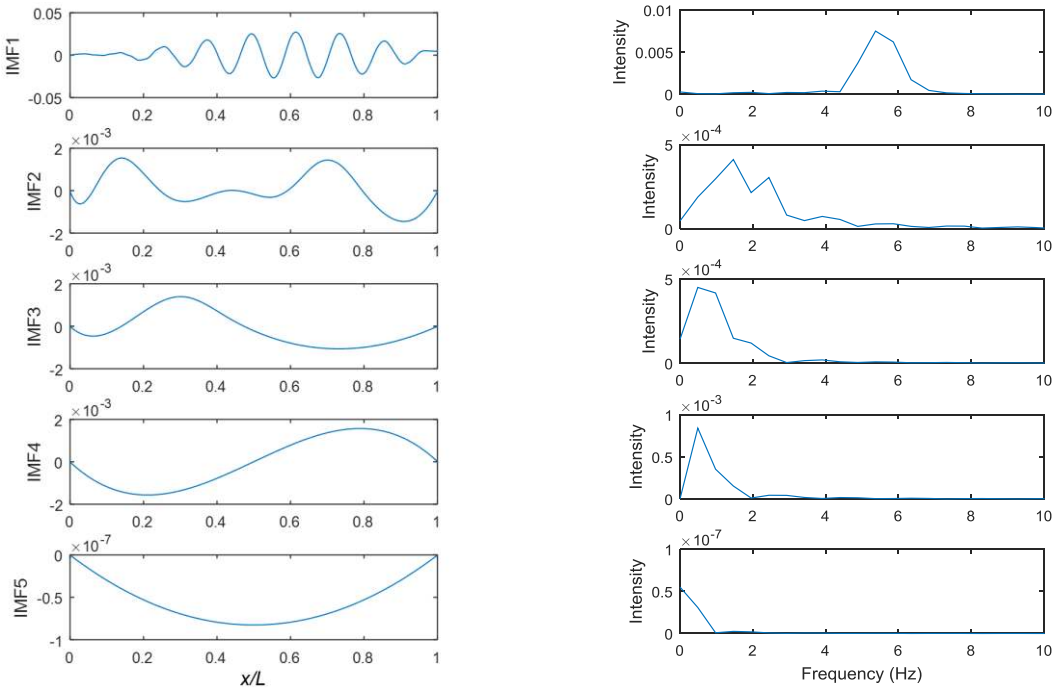

Figure 14: IMFs of the difference in the accelerations measured for the healthy and damaged cases and their FFT spectra ($x/L = vt/L$).

Fig. 14 shows the IMFs obtained from applying EMD to such a difference for the first damage case. As is clear from the frequency content of the IMFs, IMF1 corresponds to the bridge natural frequency. Thus, the other IMFs correspond to the speed pseudo-frequency component of the signal. By adding all of the IMFs except the first, the damage indicator is obtained. The results for both damage cases are shown in Fig. 15, using displacement and acceleration responses. Three crack sizes, 0.1, 0.2 and 0.3 are considered for both damage cases. There is a clear peak close to the damage location for all cases when the displacement signal is used. Fig. 15 (c) shows

that when smaller crack sizes are used, the end effect is the dominant peak while there is still a peak at the damage location.

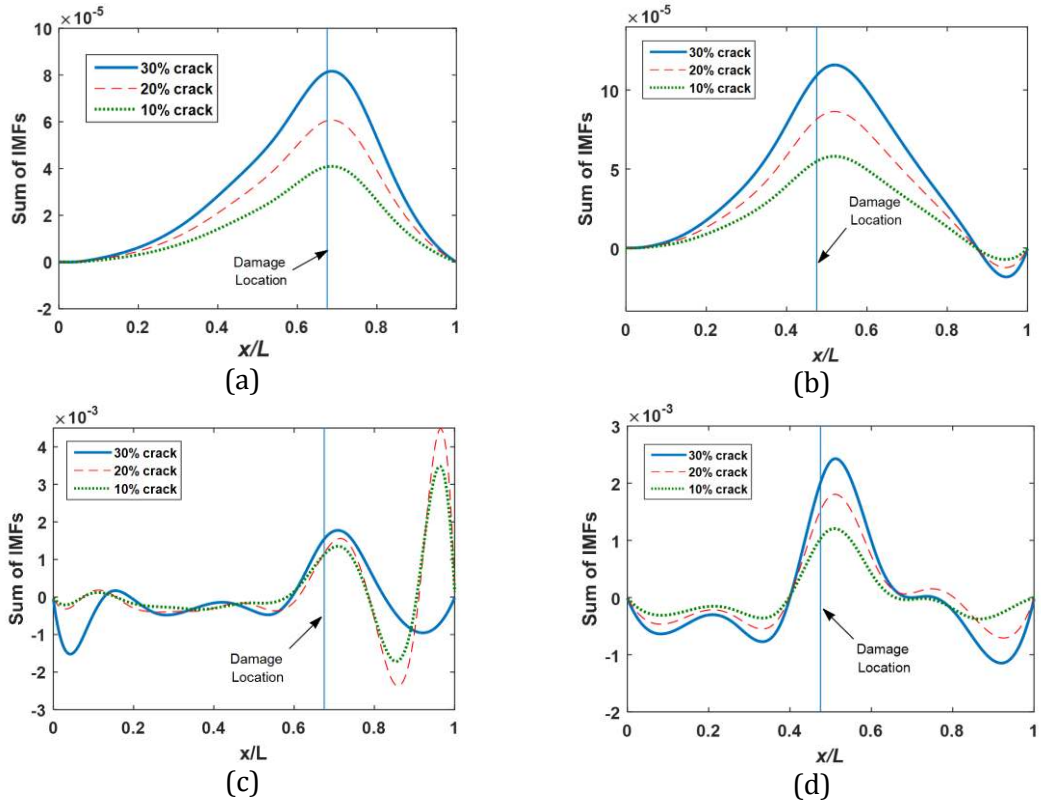

Figure 15: Speed pseudo-frequency part of the difference. (a) Damage case 1 and (b) damage case 2 using displacement. (c) Damage case 1 and (d) damage case 2 using acceleration ($x/L = vt/L$).

The test conditions for the vehicle passing over the healthy and damaged beams is assumed to be same. These conditions include the vehicle speed, the wheel path and the environmental condition (temperature) of the beam that may change when the test is repeated for the damaged case. Therefore, they need to be considered in this approach to achieve a reliable result. For the case where the vehicle speed is not perfectly constant or varies from the healthy case to the damaged one, the key point is that the speed should be measured exactly to map the vehicle response versus the location of the vehicle in terms of x/L.

3.4. Two quarter cars on a Class A road profile

A number of researchers [17, 10, 13 and 15] have reported that estimation of bridge frequency from the vehicle response is difficult when a road profile is present. In most cases, the vehicle and road profile frequencies are dominant in the vehicle response, while the bridge frequency

may be barely detectable. Yang and Chang (2009a) illustrated that with high vehicle/bridge acceleration amplitude ratios, the probability of successfully identifying the bridge frequency is less. Recently, a subtraction idea has been proposed by Yang et al. (2012) in which the effect of road profile is largely removed by subtracting the responses measured from identical following axles. Malekjafarian and Obrien (2014) show the idea of subtracting the measured acceleration responses of two following axles travelling over a bridge. It is demonstrated that the effect of road profile is substantially removed from the residual acceleration response, provided the two axles have the same properties. However, the presence of road roughness is still classified as one of the most important challenges in indirect bridge monitoring methods (Malekjafarian et al., 2015).

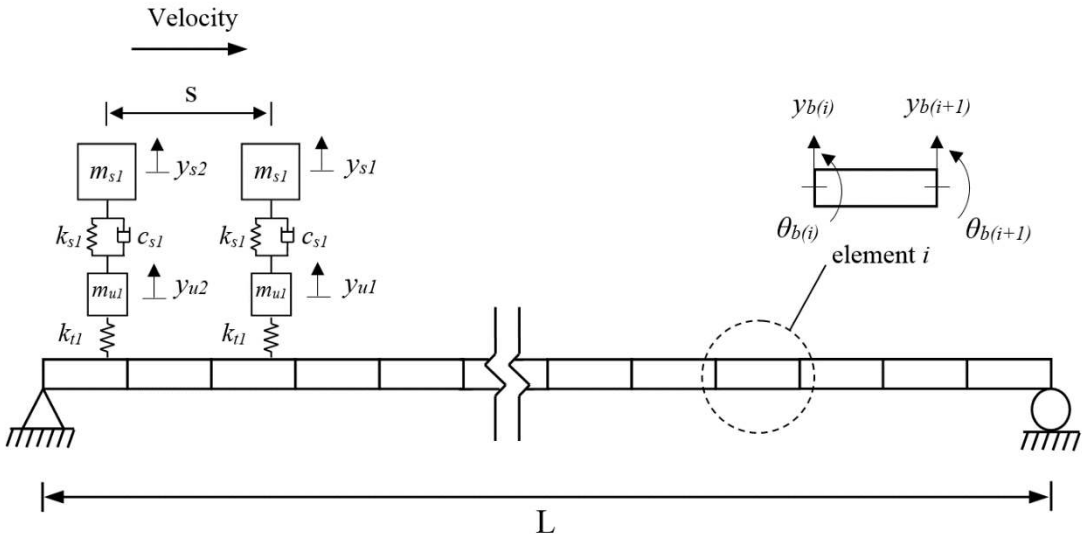

Figure 16: Two quarter cars passing over a bridge

It is suggested in this paper, that if the same vehicle is employed for the healthy and damaged cases and the same road profile exists in each case, the effect of road profile can be removed by subtracting the responses. On the other hand, when a road profile is present in the simulation, it is recommended by Li (2014) to increase the amplitude of the bridge components at least to the same level as the road profile. The amplitude of the speed pseudo-frequency part corresponds to the static load applied to the bridge (the weight of the vehicle). Therefore, in this section two following axles are modelled passing over the bridge instead of one in order to increase the total

moving load (Fig. 16). The same bridge as for Section 2 is considered, except that a road profile is added. The vehicle speed is selected to be 5 m/s in this case. The irregularities of this profile are randomly generated according to the ISO standard (1995) for a road class 'A' (very good) profile, as expected in a well maintained highway. The speed pseudo-frequency component of the difference of the responses measured on the first axle passing over healthy and damaged bridges is obtained as before. The results are shown in Fig. 17 for the two damage cases.

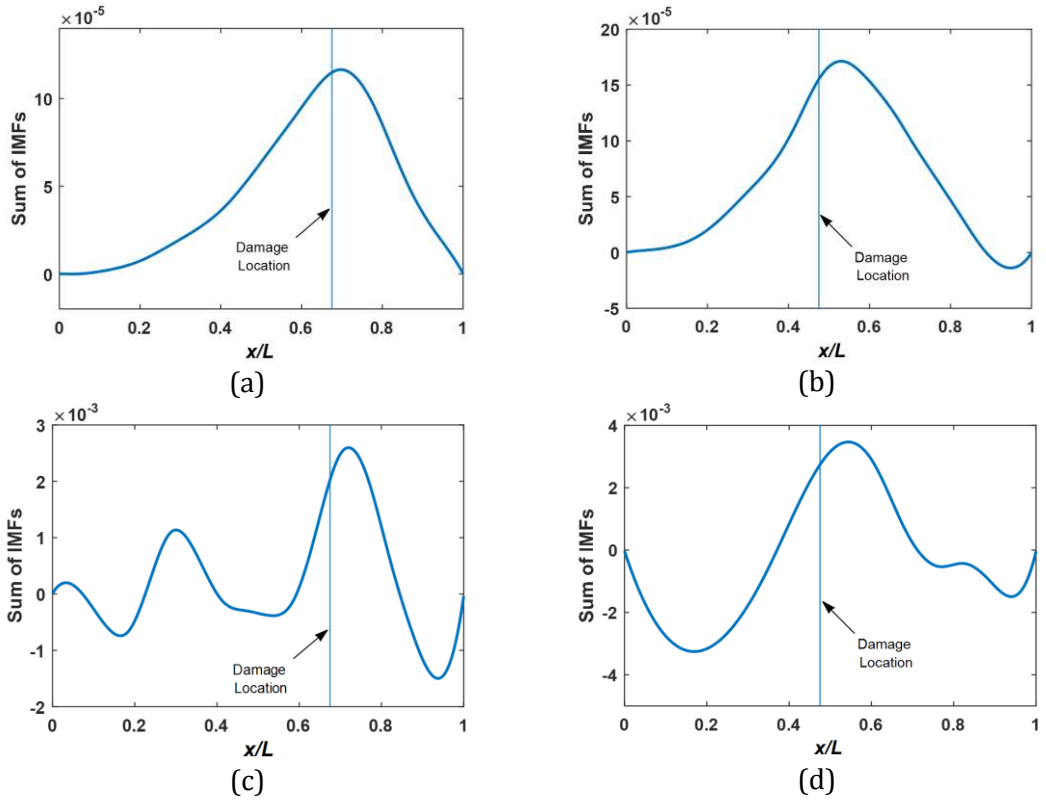

Figure 17: The speed pseudo-frequency part of the difference in the presence of a road profile. (a) Damage case 1 and (b) damage case 2 using displacement. (c) Damage case 1 and (d) damage case 2 using acceleration ($x/L = vt/L$).

Comparing Figures 15 and 17 shows that the presence of road profile causes some more oscillation in the damage indicator. However, damage can still be detected, as evidenced by the non-zero results and there are still peaks adjacent to the damage locations.

3.5. Changes in the transverse position of the vehicle on the bridge

As explained in Section 3.3 the damage indicator is based on the difference between the responses for healthy and damaged bridges. The idea relies on the assumption that the vehicle excited by the same road surface before and after occurrence of damage. Achieving this in the filed may be difficult. The vehicle may pass along a parallel track, in a slightly different transverse position on the bridge. (The surface profile may also have changed due to pavement wear. The effect would be similar.) Therefore, the sensitivity of the algorithm is tested for changes in the transverse positon of the vehicle on the bridge. A carpet if correlated profiles (Fig. 18) is generated (Cebon and Newland, 1983) from the initial road profile. It is assumed that the vehicle passes the healthy and damaged structure in different relative lateral positions, Δr.

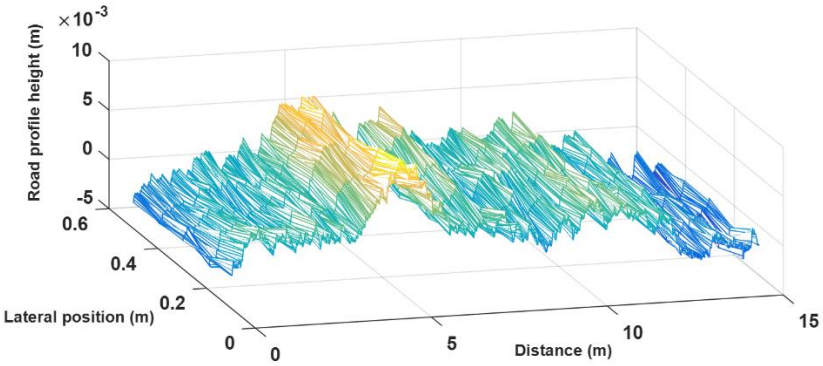

Figure 18: Carpet profile

Figs 19(a) and (b) show the damage indicator using the vehicle displcement when Δr = 0.001m and Δr = 0.01m, respectively. The results for vehicle acceleration when Δr = 0.0005m and Δr = 0.001m are shown in Fig. 19(c) and (d), respectively. It can be seen that when displacement is used, the damage indicator is less sensitive to the changes in the lateral position of the vehicle.

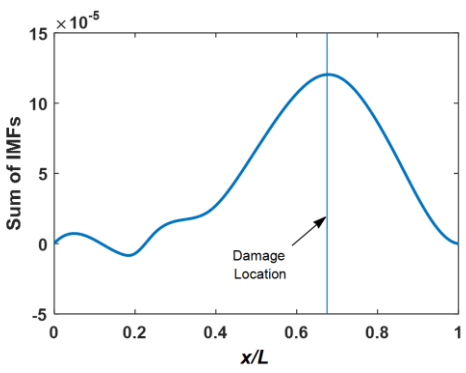

(a)

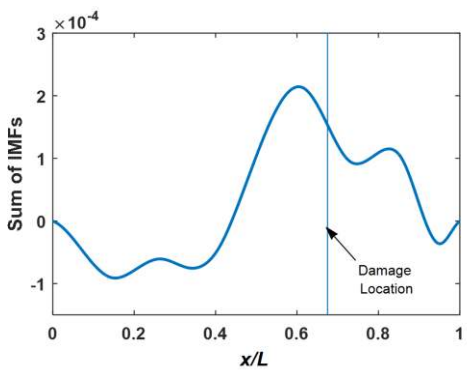

(b)

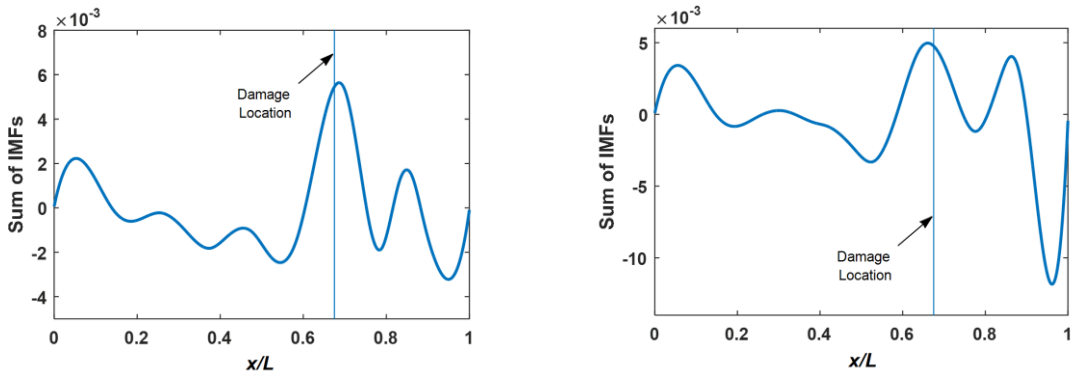

(c) (d)

Figure 19: Speed pseudo-frequency part of the difference using a range of relative positions of the vehicle on the road carpet. (a) $\Delta r = 0.001\text{m}$ and (b) $\Delta r = 0.01\text{m}$ using displacement. (c) $\Delta r = 0.0005\text{m}$ and (d) $\Delta r = 0.001\text{m}$ using acceleration ($x/L = vt/L$).

4. Conclusion

A bridge damage detection procedure using Empirical Mode Decomposition is proposed in this paper using the response measured on a passing vehicle. It is theoretically shown that the vehicle response contains three main parts and that the speed pseudo-frequency part is sensitive to damage. EMD is used to extract this part from the total response. A numerical case study of vehicle bridge interaction is modelled using the FE method to demonstrate the potential of the approach. It is shown that damage location may be identified with acceptable accuracy using the proposed method. However the method is sensitive to changes in the road profile as might be expected from changes in the the lateral position of the vehicle. It is concluded that the damage may be located by if the differences in the profile are small.

Acknowledgment

The authors wish to express their gratitude for the financial support received from Transport Infrastructure Ireland (TII) and Science Foundation Ireland towards this investigation under the US-Ireland Partnership Scheme

References

Cebon, D., 1999. Handbook of Vehicle-Road Interaction. Taylor & Francis, London and New York.

Cebon, D., Newland, D., 1983. Artificial generation of road surface topography by the inverse FFT method. Vehicle Syst Dyn 12, 160-165.

Chen, H., Kurt, M., Lee, Y.S., McFarland, D.M., Bergman, L.A., Vakakis, A.F., 2014. Experimental system identification of the dynamics of a vibro-impact beam with a view towards structural health monitoring and damage detection. Mech Syst Signal Pr 46, 91-113.

Clough, R.W., Penzien, J., 1993. Dynamics of Structures. McGraw-Hill, New York.

Fan, W., Qiao, P.Z., 2011. Vibration-based Damage Identification Methods: A Review and Comparative Study. Struct Health Monit 10, 83-111.
González, A., OBrien, E.J., McGetrick, P.J., 2012. Identification of damping in a bridge using a moving instrumented vehicle. Journal of Sound and Vibration 331, 4115-4131.
He, W., Zhu, S., 2015. Moving load-induced response of damaged beam and its application in damage localization. Journal of Vibration and Control.
Huang, N.E., Shen, Z., Long, S.R., 1999. A new view of nonlinear water waves: The Hilbert spectrum. Annu Rev Fluid Mech 31, 417-457.
Huang, N.E., Shen, Z., Long, S.R., Wu, M.L.C., Shih, H.H., Zheng, Q.N., Yen, N.C., Tung, C.C., Liu, H.H., 1998. The empirical mode decomposition and the Hilbert spectrum for nonlinear and non-stationary time series analysis. P Roy Soc a-Math Phy 454, 903-995.
ISO8608:1995, 1995. Mechanical Vibration-road Surface Profiles-reporting of Measured Data', International Standards Organisation.
Kim, C.W., Isemoto, R., McGetrick, P.J., Kawatani, M., OBrien, E.J., 2014. Drive-by bridge inspection from three different approaches. Smart Structures and Systems 13, 775-796.
Kim, C.W., Kawatani, M., 2009. Challenge for a drive-by bridge inspection, 10th International Conference on Structural Safety and Reliability ICOSSAR2009, Osaka, Japan, pp. 758-765.
Kurt, M., Chen, H., Lee, Y.S., McFarland, D.M., Bergman, L.A., Vakakis, A.F., 2012. Nonlinear system identification of the dynamics of a vibro-impact beam: numerical results. Arch Appl Mech 82, 1461-1479.
Lederman, G., Wang, Z., Bielak, J., Noh, H., Garrett, J.H., Chen, S., Kovacevic, J., Cerda, F., Rizzo, P., 2014. Damage quantification and localization algorithms for indirect SHM of bridges, in: Airong Chen, D.M.F., Xin Ruan (Ed.), Bridge Maintenance, Safety, Management and Life Extension, Shanghai, China, pp. 640-647.
Li, Z., 2014. Damage identification of bridges from signals measured with a moving vehicle. The University of Hong Kong (Pokfulam, Hong Kong).
Li, Z.H., Au, F.T.K., 2014. Damage Detection of a Continuous Bridge from Response of a Moving Vehicle. Shock and Vibration Vol. 2014.
Lin, C.W., Yang, Y.B., 2005. Use of a passing vehicle to scan the fundamental bridge frequencies: An experimental verification. Engineering Structures 27, 1865-1878.
Malekjafarian, A., McGetrick, P., OBrien, E.J., 2015. A review of indirect bridge monitoring using passing vehicles. Shock and Vibration 2015, Article ID 286139.
Malekjafarian, A., Obrien, E.J., 2014. Identification of bridge mode shapes using Short Time Frequency Domain Decomposition of the responses measured in a passing vehicle. Engineering Structures 81, 386-397.
McGetrick, P., Kim, C.A., 2014a. A Wavelet Based Drive-by Bridge Inspection System, in: Airong Chen, D.M.F., Xin Ruan (Ed.), Proceedings of the 7th International Conference on Bridge Maintenance Safety and Management, IABMAS 2014, Shanghai, China.
McGetrick, P.J., Kim, C.W., 2013. A Parametric Study of a Drive by Bridge Inspection System Based on the Morlet Wavelet. Key Engineering Materials 569, 262-269.
McGetrick, P.J., Kim, C.W., 2014b. An indirect bridge inspection method incorporating a wavelet-based damage indicator and pattern recognition, in: Cunha, A., Caetano, E., Ribeiro, P., Müller, G. (Eds.), 9th International Conference on Structural Dynamics, EURODYN 2014, Porto, Portugal.
Nguyen, K.V., Tran, H.T., 2010. Multi-cracks detection of a beam-like structure based on the on-vehicle vibration signal and wavelet analysis. Journal of Sound and Vibration 329, 4455-4465.
OBrien, E.J., Keenahan, J., 2014. Drive-by damage detection in bridges using the apparent profile. Structural Control and Health Monitoring DOI: 10.1002/stc.1721.
OBrien, E.J., Malekjafarian, A., 2015. Identification of bridge mode shapes using a passing vehicle, 7th International Conference on Structural Health Monitoring of Intelligent Infrastructure (SHMII), Italy, Turin.

OBrien, E.J., Malekjafarian, A., 2016. A mode shape-based damage detection approach using laser measurement from a vehicle crossing a simply supported bridge. Structural Control and Health Monitoring DOI: 10.1002/stc.1841.
Oshima, Y., Yamamoto, K., Sugiura, K., 2014. Damage assessment of a bridge based on mode shapes estimated by responses of passing vehicles. Smart Structures and Systems 13, 731-753.
Qiao, P.Z., Cao, M.S., 2008. Waveform fractal dimension for mode shape-based damage identification of beam-type structures. Int J Solids Struct 45, 5946-5961.
Sinha, J.K., Friswell, M.I., Edwards, S., 2002. Simplified models for the location of cracks in beam structures using measured vibration data. Journal of Sound and Vibration 251, 13-38.
Tedesco, J.W., McDougal, W.G., Ross, C.A., 1999. Structural dynamics: theory and applications. Addison Wesley Longman.
Yang, Y., Chen, W.-F., 2015. Extraction of Bridge Frequencies from a Moving Test Vehicle by Stochastic Subspace Identification. Journal of Bridge Engineering, 04015053.
Yang, Y.B., Chang, K.C., 2009a. Extracting the bridge frequencies indirectly from a passing vehicle: Parametric study. Engineering Structures 31, 2448-2459.
Yang, Y.B., Chang, K.C., 2009b. Extraction of bridge frequencies from the dynamic response of a passing vehicle enhanced by the EMD technique. Journal of Sound and Vibration 322, 718-739.
Yang, Y.B., Li, Y.C., Chang, K., 2014. Constructing the mode shapes of a bridge from a passing vehicles: a theoretical study. Smart Structures and Systems 13, 797-819.
Yang, Y.B., Li, Y.C., Chang, K.C., 2012. Using two connected vehicles to measure the frequencies of bridges with rough surface: a theoretical study. Acta Mech 223, 1851-1861.
Yang, Y.B., Lin, C.W., Yau, J.D., 2004. Extracting bridge frequencies from the dynamic response of a passing vehicle. Journal of Sound and Vibration 272, 471-493.